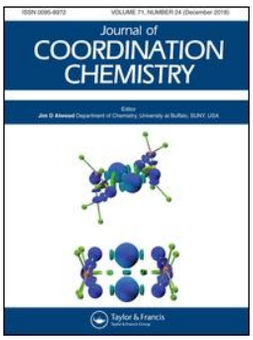

Journal of Coordination Chemistry

ISSN: (Print) (Online) Journal homepage: https://www.tandfonline.com/loi/gcoo20

Synthesis, characterization, and biological evaluation of 4-[(4-hydroxy-7-methyl-1,3-benzothiazol-2-yl) diazenyl]-5-methyl-2-phenyl-2,4-dihydro-3-pyrazol-3-one and its metal complexes

Mallikarjuna Niluvanji Matada , Keshavayya Jathi , Kiptoo Geoffry , Ravi Berenkere Nagarajappa & Harmesh Chander Tandon

To cite this article: Mallikarjuna Niluvanji Matada , Keshavayya Jathi , Kiptoo Geoffry , Ravi Berenkere Nagarajappa & Harmesh Chander Tandon (2020): Synthesis, characterization, and biological evaluation of 4-[(4-hydroxy-7-methyl-1,3-benzothiazol-2-yl) diazenyl]-5-methyl-2-phenyl-2,4-dihydro-3-pyrazol-3-one and its metal complexes, Journal of Coordination Chemistry, DOI: 10.1080/00958972.2020.1787393

To link to this article: https://doi.org/10.1080/00958972.2020.1787393

JOURNAL OF COORDINATION CHEMISTRY
https://doi.org/10.1080/00958972.2020.1787393

Taylor & Francis
Taylor & Francis Group

Synthesis, characterization, and biological evaluation of 4-[(4-hydroxy-7-methyl-1,3-benzothiazol-2-yl) diazenyl]-5-methyl-2-phenyl-2,4-dihydro-3-pyrazol-3-one and its metal complexes

Mallikarjuna Niluvanji Matada[a], Keshavayya Jathi[a], Kiptoo Geoffry[b], Ravi Berenkere Nagarajappa[a] and Harmesh Chander Tandon[c]

[a]Department of PG Studies and Research in Chemistry, School of Chemical Sciences, Jnana Sahyadri, Kuvempu University, Shankaraghatta, Shimoga, Karnataka, India; [b]Department of Chemistry and Biochemistry, School of Biological and Physical Sciences, Moi University, Eldoret, Kenya; [c]Department of Chemistry, Sri Venkateswara College, Dhula Kuan, New Delhi, India

ABSTRACT

New mononuclear Cu(II), Co(II) and Ni(II) complexes of novel azo-dye ligand 4-[(4-hydroxy-7-methyl-1,3-benzothiazol-2-yl)diazenyl]-5-methyl-2-phenyl-2,4-dihydro-3-pyrazol-3-one (L) with O,N-donor site were synthesized and are characterized by various spectroscopic techniques. The quantum chemical parameters were evaluated for all the compounds by ZINDO/1 semi-empirical method and are compared with the experimental data. Spectral investigations suggested the octahedral geometry for Co(II) and Ni(II) complexes and distorted tetrahedral geometry for Cu(II) complex. The antibacterial activity of the compounds was screened against different microbial strains and the results indicated that all the metal complexes exhibited higher activity than the free ligand. The interaction of pUC18 DNA with the synthesized compounds was explored by gel electrophoresis technique. All metal complexes exhibited significant cleavage activity against supercoiled pUC18 DNA. The anticancer activity of the compounds was studied against K562, A549, and MDA-MB-231 by MTT assay and all the metal chelates exhibited good anticancer properties.

ARTICLE HISTORY
Received 19 April 2020
Accepted 13 June 2020

KEYWORDS
Azo dyes; Benzothiazole; metal complexes; TG-DTA; DNA cleavage

CONTACT Keshavayya Jathi jathikeshavayya1959@gmail.com Department of PG Studies and Research in Chemistry, School of Chemical Sciences, Jnana Sahyadri, Kuvempu University, Shankaraghatta-577451, Shimoga, Karnataka, India

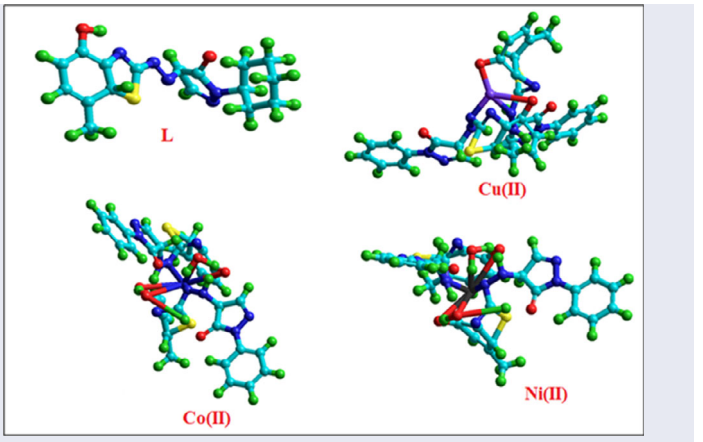

1. Introduction

Azo (-N = N-) dyes are important organic molecules and have attracted attention in both academic and applied research [1–3]. Therefore, recently several studies have been carried out on preparation and spectral properties of azo dyes. They are the most widely used class of dyes due to their versatile applications in various fields and especially in dying of textile fibers, coloring of different materials (wood, wool, leather, metal foil, and plastic), biological, and medical investigations [4]. In contrast to azobenzene dyes, the azo compounds having hetero atoms in a ring exhibiting brilliant color and chromophoric strength. Usually, the -N = N- in the azo-dye undergoes reversible cis-trans isomerization and because of their good thermal stability they can be used in the design of photo-switches [5, 6].

Substituted benzothiazoles containing azo-group were found to be useful in the design of optical data storage devices [7], dye-sensitized solar cells [8], and dying of textile fibers [9–11]. In recent decades, the most important step in the development of coordination chemistry was the synthesis of new ligands with a unique identity and novel reactivity. Metal complexes of azo-dyes are reported to be involved in a number of metabolic reactions such as inhibition of RNA and DNA, protein synthesis, carcinogenesis and nitrogen fixation. In addition, azo compounds and their metal complexes are used in analytical chemistry as indicators in acid-base, redox, and complexometric titrations [12].

In continuation of our work in the field of coordination chemistry of transition metal (Cu, Co and Ni) chelates with heterocyclic azo dyes and in the light of the fact that azo metal chelates possess excellent pharmacological properties [13–20]. In the present work, we have made an attempt to synthesize novel metal complexes of the azo-dye ligand, 4-[(4-hydroxy-7-methyl-1,3-benzothiazol-2-yl)diazenyl]-5-methyl-2-phenyl-2,4-dihydro-3-pyrazol-3-one (L). The chemical structures of the synthesized compounds were deduced from the analytical and spectroscopic techniques. The antimicrobial, DNA-cleavage and anticancer studies were carried out to explore the pharmacological properties of the newly synthesized compounds.

2. Experimental

2.1. Analysis and physical measurements

Spectral studies were carried out for the ligand and its metal complexes. Elemental analysis (C, H, and N) was performed on a Vario EL III CHNS analyzer. IR spectra of the newly synthesized compounds were recorded as KBr pellets on a Perkin-Elmer spectrum RX-IFTIR instrument in the region 4000–200 cm^{-1}. The ^{1}H NMR spectrum of the ligand was recorded on a Bruker Avance II, 400 MHz using DMSO-d_6 as a solvent. ESI-MS were recorded on a mass spectrometer equipped with electrospray ionization (ESI) source having a mass range 4000 amu in quadruple and 20,000 amu in Tof. The UV-Vis spectra of the compounds were recorded on an Elico-SL 164 double-beam spectrometer in the range 200–800 nm using 10^{-6} M solution in DMSO. The room temperature ESR spectrum of the Cu(II) complex in the polycrystalline state was recorded on a BRUKER Bio Spin Gmbh spectrometer at a microwave frequency 8.75–9.65 GHz. The experiment was carried out using diphenylpicrylhydrazyl (DPPH) as reference with field set at 3000 Gauss. The molar conductivity measurements were recorded on an ELICO CM-180 conductivity bridge in dry DMSO (10^{-6} M) solution using a dip-type conductivity cell fitted with a platinum electrode. The thermal analysis (TG-DTA) of the complexes were investigated from room temperature to 750 °C in nitrogen atmosphere on a Perkin Elmer STA 6000 thermal analyzer with rate of heating of 20 °C min^{-1} and magnetic susceptibility measurements were carried out at room temperature on a vibrating sample magnetometer (VSM) using Ni as calibrant. Further, the molecular geometries of the azo dye and its complexes were optimized by quantum chemical method using ZINDO/1 (semi empirical calculation) method and the quantum chemical parameters were evaluated for all the studied compounds.

2.2. Reagents and synthetic methods

All chemicals used for the synthesis were of AR grade, purchased commercially. All solvents were purified by distillation and used. Bromine, potassium thiocyanate, sodium nitrite, and glacial acetic acid were purchased from Sigma Aldrich chemical company, India. Melting points of the newly synthesized compounds were determined by electro-thermal apparatus using open capillary tubes and are uncorrected. The metal contents of the complexes were determined as per the standard procedures [21]. The purity of the compounds was checked by thin layer chromatography (TLC) and the spots were observed in iodine vapor. The starting material 2-amino-7-methyl-1,3-benzothiazol-4-ol was prepared by the literature method [22, 23] and 5-methyl-2-phenyl-2, 4-dihydro-3*H*-pyrazol-3-one was purchased from Sigma Aldrich.

2.2.1. Synthesis of azo dye ligand (L)

A well stirred solution of 2-amino-7-methyl-1,3-benzothiazol-4-ol (2 mmol) in 6 mL conc. HCl was cooled in an ice bath and diazotized with the solution of sodium nitrite (2.2 mmol) in 2 mL of H_2SO_4. The resulting mixture was stirred for 2 h at 0–5 °C. The

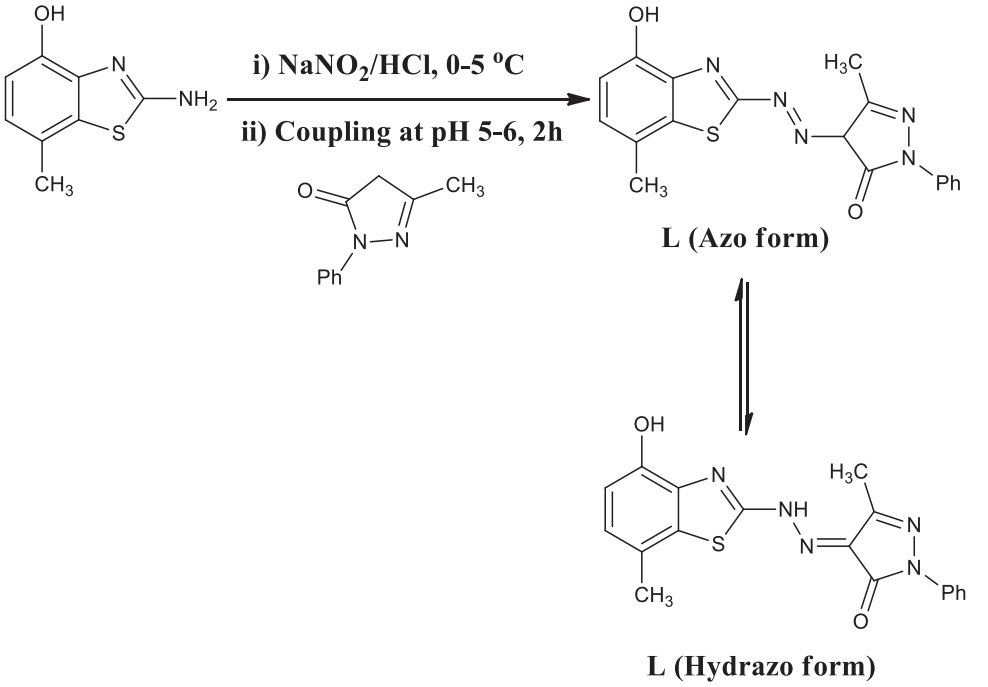

Scheme 1. Synthesis of azo dye ligand (L).

cold diazonium salt solution was added to the well-cooled solution of 5-methyl-2-phenyl-2,4-dihydro-3*H*-pyrazol-3-one (2 mmol) in acetic acid (10 mL). The reaction mixture was stirred for another 2 h at 0–5 °C maintaining the pH 6 by adding the required volume of sodium carbonate solution. The crude product was filtered off, washed with hot water, dried, and recrystallized from ethanol (Scheme 1).

2.2.2. Synthesis of Cu(II), Co(II), and Ni(II) complexes

To the hot solution of (0.2 g, 0.00054 mol) 4-[(7-hydroxy-4-methyl-1,3-benzothiazol-2-yl)diazenyl]-5-methyl-2-phenyl-2,4-dihydro-3*H*-pyrazol-3-one (L) in methanol (5 mL) was added to a hot methanolic solutions of respective metal salts (0.0002 mol) and refluxed on a water bath for about 5–6 h. The whole reaction mixture was cooled to room temperature and poured into distilled water. The colored solids separated were collected by filtration, washed with sufficient quantity of distilled water, and then with hot ethanol to remove any impurities. It was finally dried over anhydrous $CaCl_2$ in a vacuum desiccator.

2.3. Pharmacological activity

2.3.1. Antibacterial assay

The antibacterial activity of the synthesized compounds was performed in agar well-diffusion method explained by Murray and coworkers [24]. Nutrient agar was poured into the Petri dish and allowed to solidify. Overnight grown bacterial strains *Klebsiella*

pneumoniae (13883), *Escherichia coli* (ATCC 25922), and *Bacillus subtilis* (ATCC 19659) were seeded on to petri plates and wells of 6.0 mm diameter were aseptically bored. Synthesized compounds of 50 μL were dissolved in DMSO of (1.5, 3.0 mg mL^{-1}) were added into the wells. The petri dish plates were kept for incubation for 24 h at 37 °C. The antimicrobial activity was assessed as inhibition zones flanging the wells. Negative control used was DMSO and tetracycline as positive control.

2.3.1.1. Absorbance-based microtiter plate assay (MPA). Microtiter plate assay was performed as previously described [25, 26]. Sterile growth media of 100 μL was pipetted into a microtiter plate and to it, 100 μL aliquot of synthesized compounds were then diluted two-fold in each well. Finally, 100 μL of the culture media of optical density (0.5) at 600 nm were added to all the wells. Positive controls contained growth media inoculated with microorganisms. Negative controls contained synthesized compounds and sterile growth media only. The plates were incubated for 24 h at 37 °C and absorbance was recorded at 600 nm.

2.3.2. DNA-cleavage activity

The cleavage of supercoiled plasmid pUC18 DNA by all the synthesized compounds was carried out by gel electrophoresis method [27, 28]. This movement is retarded when they are bound to other molecules. In a typical experiment, 200 mg of agarose was dissolved in 25 mL of Tris-acetate (TAE) buffer (4.84 g Tris base, pH 8.0, 0.5 M EDTA) by boiling. When the gel attains approximately 55 °C, it was poured into the gel cassette fitted with a comb. The gel was allowed to solidify and then carefully the comb was removed. The gel was placed in the electrophoresis chamber flooded with TAE buffer. The synthesized compounds were dissolved in freshly distilled DMSO (1 mg mL^{-1}). The test compounds were added separately to the isolated pUC18 DNA (225 ng) and incubated for 2 h at 37 °C. After incubation, 20 μL of DNA sample (mixed with bromophenol blue dye at 1:1 ratio) was loaded carefully into the wells, along with standard DNA marker and a constant electricity of 50 V was passed for around 45 min. The gel was removed and carefully strained with ethidium bromide (ETBR) solution (10 μg mL^{-1}) for 10–15 min. The bands were observed under UV trans-illuminator (UVP, Germany) and photographed to determine the extent of DNA-cleavage, and the results were compared with those of a standard DNA marker.

2.3.3. Cytotoxic studies

The cytotoxic study of the newly synthesized metal chelates was investigated by MTT assay against human mammary tumor cell line (MDA-MB-231), human lung carcinoma cell line (A549) and human chronic myeloid leukemia cell line (K562) which were previously procured from the National Centre for Cell Science (NCCS), Pune, India. The cancer cell lines used in this study were subcultured in Leibovitz's L-15, Ham's F-12K and RPMI 1640 medium, respectively. The antibiotics like 2 mM L-glutamine (Thermo Fisher Scientific, Inc.; Waltham, MA, USA) containing 10% FBS (Gibco; Grand Island, NY, USA) and 1% by volume penicillin/streptomycin (Invitrogen Life Technologies; Carlsbad, CA, USA) were added to the above medium containing cell lines and these cell were incubated in 5% humidified incubator 37 °C. The inhibition effect of the

Table 1. Physical, analytical, and molar conductance data of azo dye ligand (L) and its metal complexes.

Ligand/Complexes		Mol. formula	M.W.	m.p. (°C)	Color	Elemental analysis C	H	N	M	Δ_o $cm^2\Omega^{-1}$ mol^{-1}
1	L	$C_{18}H_{15}N_5O_2S$	365.40	267	Orange red	59.16 (59.22)	4.14 (4.19)	19.17 (19.26)	–	–
1a	$[Cu(L)_2]$	$C_{36}H_{28}CuN_{10}O_4S_2$	792.34	328	Dark blue	54.57 (53.31)	3.56 (3.48)	17.68 (17.51)	8.02 (7.98)	25
1b	$[Co(L)_2(H_2O)_2]$	$C_{36}H_{32}CoN_{10}O_6S_2$	823.76	322	Red	52.49 (52.34)	3.92 (3.32)	17.00 (16.78)	7.15 (7.13)	23
1c	$[Ni(L)_2(H_2O)_2]$	$C_{36}H_{32}NiN_{10}O_6S_2$	823.52	325	Brown	52.50 (52.41)	3.92 (3.46)	17.01 (16.79)	7.79 (7.66)	19

Table 2. Important IR absorption bands of azo dye ligand (L) and its metal complexes (cm^{-1}).

Ligand/Complexes		$\upsilon(H_2O)$	$\upsilon(OH)_{phenolic}$	$\upsilon(C=O)_{carbonyl}$	$\upsilon(N=N)_{azo}$	$\upsilon(C\text{-}O)_{phenolic}$	υ(M-N)	υ(M-O)
1	L	–	3361	1647	1551	1218	–	–
1a	$[Cu(L)_2]$	–	–	1665	1464	1291	476	576
1b	$[Co(L)_2(H_2O)_2]$	3175	–	1658	1498	1262	471	564
1c	$[Ni(L)_2(H_2O)_2]$	3350	–	1646	1462	1330	479	577

target compounds was determined by 3-(4,5-dimethylthiazolyl-2)-2,5-diphenyltetrazolium bromide (MTT) assay as discussed in earlier reports [29, 30]. Cisplatin was used as a positive control (standard) and DMSO as a negative control. The results of the study were presented in the form of IC_{50} values and they are discussed in the Results and Discussion section.

3. Results and discussion

3.1. Chemistry

The synthetic path employed to obtain the target compounds are depicted in Scheme 1. The azo dye ligand (L) and its metal complexes have been synthesized and characterized by physicochemical methods. All the prepared metal complexes are colored solids, non-hygroscopic, stable at room temperature and possess high melting point ($> 300\,^{\circ}C$). The metal complexes are freely soluble in DMF and DMSO but insoluble in common other organic solvents. Elemental analysis and analytical data of the complexes (Table 1) suggest that the metal to ligand ratio (M:L) of the complexes is 1:2 stoichiometry of the type $[M(L)_2]$ for Cu(II) complex and $[M(L)_2(H_2O)_2]$ for Co(II) and Ni(II) complexes. The measured molar conductance values of the metal complexes were too low to account for any dissociation of the complexes in DMSO (19–25 ohm^{-1} cm^2 mol^{-1}), indicating their non-electrolytic behavior [31].

3.2. IR spectral data

The important IR absorption bands of the ligand and its metal complexes are displayed in Table 2. In the azo dye ligand (L), the absorption band at 3361 cm^{-1} is assigned to phenolic OH. A strong band at 1647 cm^{-1} is due to carbonyl function

υ(C = O). The absorption due to aromatic and aliphatic C-H stretching in the ligand can be identified by the bands at 3067 cm^{-1} and 2921 cm^{-1}, respectively. A band at 1551 cm^{-1} corresponds to azo (–N = N–) group present in the azo dye [32, 33].

The absorption due to phenolic –OH disappeared in the IR spectra of all the metal complexes of the ligand, indicating the formation of bonds between metal ion and phenolic oxygen atom through deprotonation. This was further confirmed by the enhancement of absorption frequency of the phenolic C-O bond in the region 1291–1330 cm^{-1} in all the metal complexes, suggesting the bonding of ligand through a deprotonated $(C\text{-}O)^-$ group to the metal ion [34]. In the IR spectra of the metal complexes, medium intensity weak absorption bands observed in the region 1647–1665 cm^{-1} were due to carbonyl function (C = O), which appeared almost at the same position as in the case of ligand, thus confirming the non-involvement in coordination. The absorption frequency of azo (N = N) group in all the metal complexes of the ligand shifted to lower frequency by 60–89 cm^{-1}, indicating the involvement of nitrogen atom of azo group in complexation with the metal ions. The bonding between the metal ions and the ligand was further confirmed by the appearance of new weak intensity bands in the region 564–577 cm^{-1} and 471–479 cm^{-1} in all the complexes, which are assigned to frequencies of ν(M-O) and ν(M-N) stretching vibrations, respectively [35]. The absorption bands at 3175 and 3350 cm^{-1} indicate the presence of coordinated water molecules in the Co(II) and Ni(II) complexes of the ligand (L), respectively [36–38].

3.3. ^{1}H NMR spectral studies

The ^{1}H NMR spectrum of the azo dye ligand (L) was recorded in DMSO-d_6 at room temperature. The ^{1}H NMR spectrum of the ligand exhibited a singlet at 13.50 ppm, indicating the presence of hydrazone (NH) proton [39, 40]. The signal due to phenolic -OH proton of the benzothiazole moiety resonated at 11.01 ppm; the signals due to seven aromatic protons have resonated as multiplets in the region 6.73–9.39 ppm. Six protons of two methyl groups attached to phenyl and pyrazole ring have resonated as singlets at 2.35 and 2.41 ppm, respectively.

3.4. ESI-mass spectral data

Azo dye ligand (L) and its metal complexes were studied for their mass spectral studies. The ESI-mass spectra of all the above compounds exhibited molecular ion peaks equivalent of their molecular mass along with other fragment ion peaks. The mass spectrum of the ligand exhibited M + 1 peak at 366 and 367 (100% and 19%, respectively) which is also a base peak. The mass spectra of Cu(II), Co(II), and Ni(II) complexes showed peaks attributed to the molecular ions m/z at 790, 822, and 822 corresponding to their molecular weights at 792.34, 823.76, and 823.52, respectively. Hence, the mass spectral data was found to be in good agreement with the proposed molecular structures of the compounds.

Table 3. Electronic spectral data of ligand (L) and its metal complexes.

Ligand/Complexes		Wavenumber (in cm^{-1})	Assignment	μ_{eff} (BM)	Geometry
1	L	22321	n→π^*	–	–
1a	$[Cu(L)_2]$	27624	$^2B_{1g} \rightarrow {}^2A_{1g}$	1.91	Distorted tetrahedral
		19801			
		31347			
1b	$[Co(L)_2(H_2O)_2]$	22123	$^4T_{1g}(F) \rightarrow {}^4T_{2g}(P)(\upsilon_3)$	3.98	Octahedral
		26246	$^4T_{1g}(F) \rightarrow {}^4A_{2g}(F)(\upsilon_2)$		
1c	$[Ni(L)_2(H_2O)_2]$	29940	$^3A_{2g} \rightarrow {}^3T_{1g}(P)$ (υ_3)	3.01	Octahedral
		20202	$^3A_{2g} \rightarrow {}^3T_{1g}(F)$ (υ_2)		

Table 4. ESR spectral data of Cu (II) complex of azo dye ligand (L).

Complex		$g_{\|\|}$	$g_{\perp}$	g_{av}	G
1a	$[Cu(L)_2]$	2.341	2.079	2.166	4.31

3.5. Electronic spectral studies

The UV-Visible spectra were recorded in DMSO (10^{-6} M) at room temperature. The electronic spectral data of the ligand and its complexes are presented in Table 3. The electronic spectrum of the Cu(II) complex shows three absorption bands at 19,801 cm^{-1} and 27,624 cm^{-1} and 31,347 cm^{-1} due to $^2B_{1g} \rightarrow {}^2A_{1g}$ transitions. These transitions suggest a distorted tetrahedral geometry, which is in agreement with the literature value [41, 42]. Further, this was confirmed by magnetic susceptibility measurements and it was found to be 1.91 BM, which is in good agreement with the reported value for distorted tetrahedral environment [43–45]. The electronic spectrum of Co(II) complex displayed two absorption bands at 22,123 cm^{-1} and 26,246 cm^{-1}. These bands are assigned to $^4T_{1g}$ (F) → $^4A_{2g}$ (F) (υ_2) and $^4T_{1g}$ (F) → $^4T_{2g}$ (P) (υ_3) transitions, respectively. The above transitions suggest an octahedral geometry for Co(II) complex. The magnetic moment value 3.98 BM corresponds to high spin octahedral geometry. The Ni(II) complex of the azo dye ligand under present study exhibited two bands in the region 20,202 cm^{-1} and 29,940 cm^{-1} which are assigned to $^3A_{2g} \rightarrow {}^3T_{1g}$ (F) (υ_2) and $^3A_{2g} \rightarrow {}^3T_{1g}$ (P) (υ_3) transitions. The Ni(II) complex has the magnetic moment value of 3.01 BM. Thus, the absorption bands and the magnetic moment value support an octahedral geometry for the Ni(II) complex [46–48].

3.6. ESR spectral study of Cu(II) complex

Room-temperature ESR spectrum of the Cu(II) complex in polycrystalline state was recorded in DMSO and the spin Hamiltonian parameters of the complex has been calculated and displayed in Table 4. The observed data $g_{||}(2.341) > g_{\perp}(2.079) > 2.0023$ suggest the unpaired electron lies in the d_{x2-y2} orbital in distorted tetrahedral geometry [42]. The exchange interaction between two Cu(II) centers can be explained using the Hathaway expression $G = (g_{||} - 2)/(g_{\perp} - 2)$. If $G > 4$, the exchange interaction between Cu(II) centers in the solid complex is negligible, while a value of $G < 4$ a considerable exchange interaction is indicated in the solid complex. In the present study, the value of $G = 4.31$ indicates that there is no exchange interaction in the Cu(II) complex of the ligand. Further, the mononuclear nature of the complex was supported by

Table 5. Thermal data of the metal complexes of the azo dye ligand (L).

		% Weight loss		% Metal oxide		
Complex No.	Decomposition temp. (°C)	Obsd.	Anal. Calcd	Obsd.	Anal. Calcd	Proposed mode of degradation
[Cu(L)2]	216	3.45	3.78	–	–	Loss due to two methyl groups of benzothiazole ring
	320	51.87	50.75	–	–	Loss due to two moles of $C_{10}H_9N_4O$ fragment
	464	34.42	34.12	–	–	Loss due to two molecules of benzothiazole moiety (C_7H_5NS)
	>712	–	–	10.23	10.03	CuO
$[Co(L)_2(H_2O)_2]$	110	4.91	4.37	–	–	Loss due to two coordinated water molecules
	310	7.64	7.29	–	–	Loss due to four methyl groups
	487	26.50	26.25	–	–	Loss due to two phenyl groups of pyrazole moiety and two azo groups
	696	48.63	48.80	–	–	Loss due to two moles of $C_7H_5N_3O_2S$ fragment
	>739	–	–	12.32	13.46	CoO + 3C
$[Ni(L)_2(H_2O)_2]$	162	4.29	4.37	–	–	Loss due to two coordinated water molecules
	300	23.25	22.37	–	–	Loss due to two phenyl groups of pyrazole ring and two methyl groups of benzothiazole moiety
	448	38.15	39.14	–	–	Loss due to $C_7H_3N_3S$ fragment
	583	24.23	25.52	–	–	Loss due to remaining organic moiety
	>732	–	–	10.08	9.06	NiO

the absence of a band corresponding to the transition $\Delta Ms = \pm 2$ in the observed ESR spectrum of the Cu(II) complex [49].

3.7. Thermal studies

The thermal study of the copper, cobalt, and nickel complexes of the ligand (L) was measured from ambient temperature up to 740 °C by thermogravimetric (TG) and differential thermal analysis (DTA) in an inert atmosphere at heating temperature 20 °C min^{-1}. The proposed stepwise thermal decomposition of the complexes with respect to temperature and the formation of respective metal oxides are presented in Table 5.

From the TG/DTA curve of the Cu(II) complex, the first step of decomposition stage was observed in the range of 216–320 °C with the mass loss of 3.45% (Anal. Calcd 3.78%). This may be attributed to the loss of two methyl groups of benzothiazole ring. The DTA curve exhibits an endothermic peak at 291 °C (the maximum peak temperature, T_{max}). The second step of decomposition occurs within the temperature range of 320–464 °C with the practical weight loss of 51.87% (Anal. Calcd 50.75%) which corresponds to the loss of two moles of $C_{10}H_9N_4O$ fragment. The DTA curve gives an exothermic peak at 334.34 °C. Finally, the complex underwent the third step of decomposition with a weight loss of 34.42% (Anal. Calcd 34.12%) due to loss of two moles of benzothiazole moiety (C_7H_5NS) in the temperature range 464–712 °C. Thereafter, the complex showed a gradual decomposition up to 712 °C and onwards due to the loss of remaining organic moiety and finally leaving the residue as CuO.

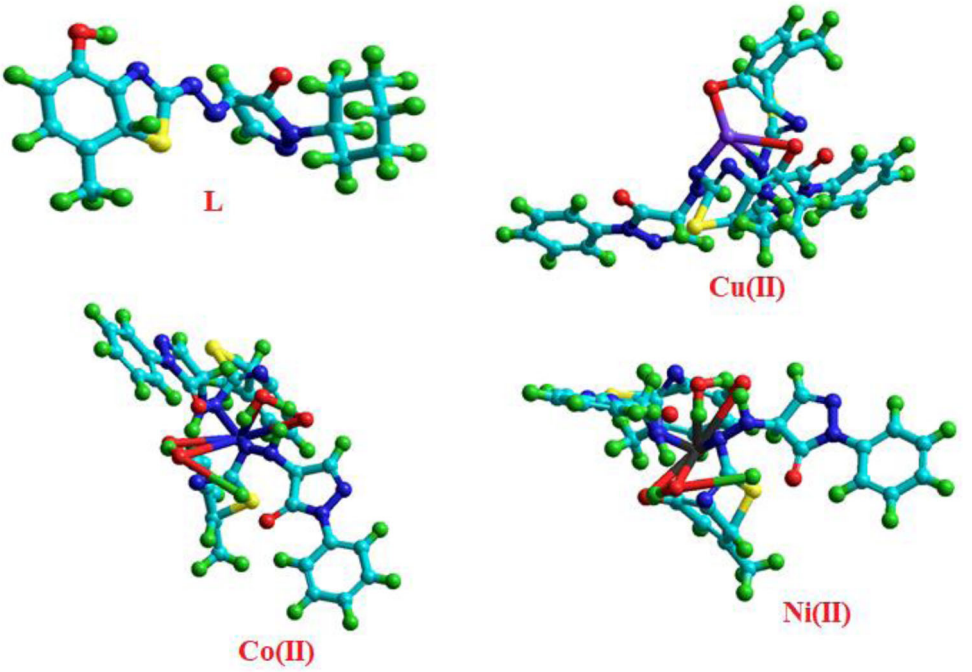

Figure 1. The optimized molecular geometries of the ligand (L) and its complexes.

In the TG/DTA curve of the Co(II) complex, four degradation steps were observed. The first degradation step with estimated mass loss 4.91% (Anal. Calcd 4.37%) within the temperature range 25–100 °C may be attributed to the loss of two coordinated water molecules. An endothermic peak in this region with T_{max} = 79.27 °C on the DTA curve. The second degradation step occurs within the temperature range 100–310 °C with a practical weight loss of 7.64% (Anal. Calcd 7.29%), corresponding to the loss of four methyl groups. The DTA curve gives an endothermic peak T_{max} = 300.87 °C. The third stage of degradation proceeds within the temperature range 310–487 °C with an estimated mass loss of 26.50% (Anal. Calcd 26.25%); an exothermic peak (T_{max} = 437.12 °C) may be attributed to the loss of two moles phenyl groups of the pyrazole ring along with azo group. The final step of the degradation was observed in the temperature range 487–696 °C with a mass loss of 48.63% (Anal. Calcd 48.80%) accompanied by an endothermic peak at T_{max} = 532.32 °C in DTA. In this step, all other organic residues (two moles of $C_7H_5N_3O_2S$ fragment) were removed from the structure leaving three carbon atoms and cobalt oxide (CoO) as the final product.

In the thermogram of the Ni(II) complex, the first stage of decomposition occurs within the temperature range of 162–300 °C with a practical weight loss of 4.29% (Anal. Calcd 4.37%) corresponding to the elimination of two coordinated water molecules. The DTA curve gives an endothermic peak at T_{max} = 263.68 °C. The resultant complex underwent further decomposition with weight loss of 23.25% (Anal. Calcd 22.37%) due to loss of two phenyl groups of the pyrazole moiety and two methyl groups of benzothiazole ring within the temperature range 300–448 °C. An endothermic peak in this region with T_{max} = 401.25 °C on the DTA curve. The third step of

Table 6. The HOMO and LUMO energy state of the ligand (L) and its complexes.

Compounds	Structure of HOMO	Structure of LUMO
L	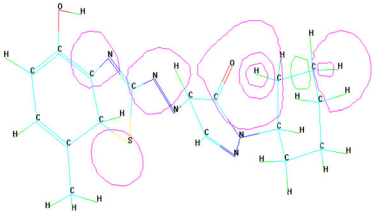	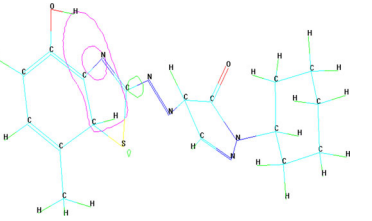
$[Cu(L)_2]$	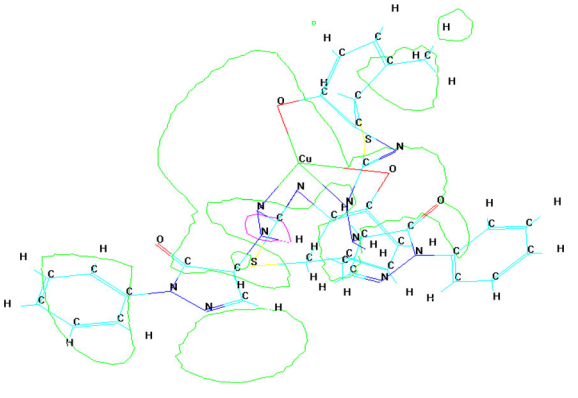	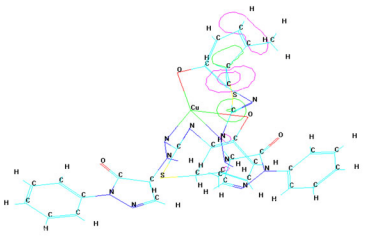
$[Co(L)_2(H_2O)_2]$		

(*continued*)

Table 6. Continued.

Compounds	Structure of HOMO	Structure of LUMO
	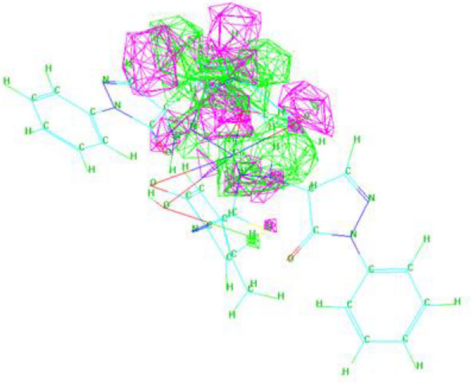	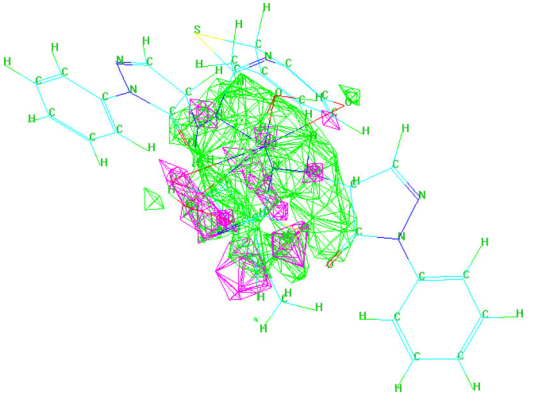
$[Ni(L)_2(H_2O)_2]$	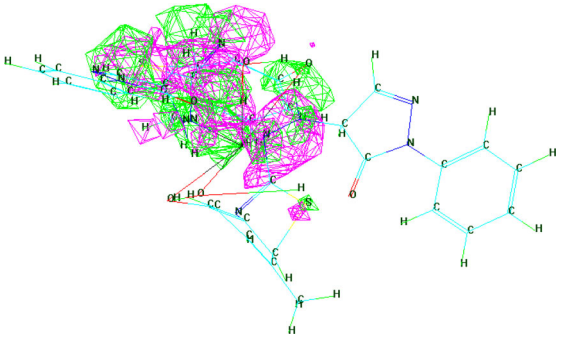	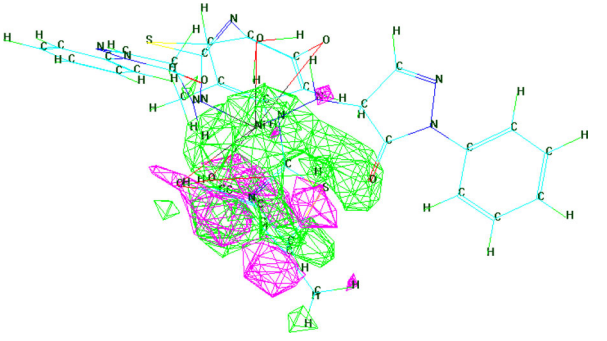

Table 7. The quantum chemical parameters evaluated for the azo dye ligand (L) and its metal complexes.

Electronic parameters	L	$[Cu(L)_2]$	$[Co(L)_2(H_2O)_2]$	$[Ni(L)_2(H_2O)_2]$
E_{HOMO} (eV)	4.58	3.21	4.46	4.19
E_{LUMO} (eV)	−5.26	−5.00	−4.54	−4.70
$E_{HOMO} - E_{LUMO}$ (eV)	9.84	8.21	9.00	8.89
Electronegativity (χ)	0.68	1.79	0.04	0.25
Chemical potential (α)	−0.68	−1.79	−0.04	−0.25
Hardness (η)	9.84	8.21	4.50	4.44
Electrophilicity index (ω)	0.02	0.19	0.0001	0.007
Ionization potential (A)	−4.58	−3.21	−4.46	−4.19
Electron affinity (I)	5.26	5.00	4.54	4.70
Dipole moment (D)	4.15	18.52	11.34	11.47

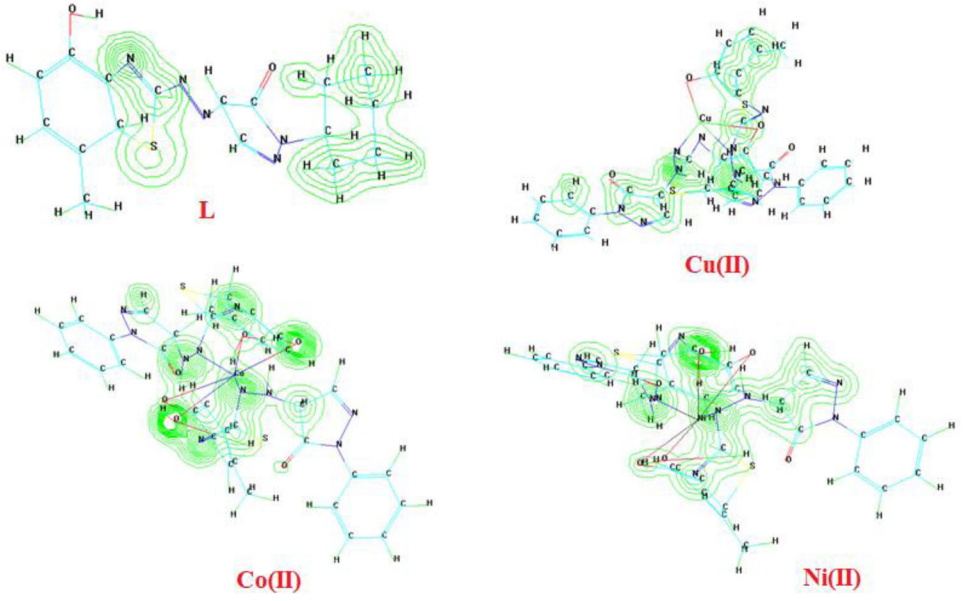

Figure 2. The picture showing the total charge density on the ligand (L) and its complexes.

decomposition with estimated weight loss of 38.15% (Anal. Calcd 39.14%) within the temperature range of 448–583 °C was accompanied by an endothermic peak at T_{max} = 527.41 °C in DTA. Further, the complex underwent decomposition within the temperature range 448–583 °C with a mass loss of 24.23% (Anal. Calcd 25.52%). Thereafter, the complex showed a gradual decomposition up to 732 °C with a loss of remaining organic moiety. The final mass of the residue corresponds to the weight of NiO.

3.8. Geometry optimization

Nowadays, the theoretical modeling used to correlate or to compare the experimentally obtained results becomes more common. This is often more useful in understanding the various structural, optical, thermal, biological, and electrochemical properties based on the difference between the highly occupied molecular orbital (HOMO) and

Table 8. Minimum inhibitory concentration (MIC, in μg mL^{-1}) of ligand (L) and its metal complexes.

Compounds		Bacterial strain		
		E. coli	*K. pneumoniae*	*B. subtilis*
1	L	19.50	12.50	13.00
1a	$[Cu(L)_2]$	31.25	15.62	16.22
1b	$[Co(L)_2(H_2O)_2]$	33.18	13.25	12.26
1c	$[Ni(L)_2(H_2O)_2]$	41.06	14.26	16.06
Tetracycline		35.06	9.53	9.53

least unoccupied molecular orbital (LUMO). As from the basic concept of the molecular orbital theory, if the energy gap between the ground state and exited state or the difference between HOMO and LUMO is small, the promotion of electron becomes easy and the molecule can be considered as more reactive and kinetically unstable. If the energy gap between HOMO and LUMO is higher, the energy required promoting a valence electron becomes high and thus the molecule becomes kinetically stable and less reactive [50]. Based on this simple concept and with the help of quantum chemical approach, one can predict and interpret the structural reactivity of the molecules. As we know from the literature, the structural and chemical variations can significantly impact the biological, electrochemical, and optical properties of the molecules. Therefore, in this study we attempted to correlate the structural properties with the biological activities. From the preliminary analysis of the theoretical results, when the molecular system approaches the lowest energy or in other words the molecule has lowest ΔE has more affinity to exhibit biochemical properties. If the molecular system has higher ΔE value, the excitation of the electron from HOMO to LUMO is difficult and shows stable or less affinity towards any chemical reaction. Hence, by calculating the ΔE from this study becomes more useful in understanding the chemical and biological properties of the newly synthesized molecules. Therefore, the geometrical structures of the synthesized azo dye and its complexes were optimized with the help of semi empirical method (ZINDO1) using Hyperchem software. The corresponding optimized geometries of the compounds are displayed in Figure 1. Further, the HOMO and LUMO energy states of each molecule were obtained from the above method and are also summarized in Table 6. The chemical and biological properties of the compounds can be studied by the quantum chemical parameters which are described by the following formulas (1–7) and the obtained values are tabulated in Table 7. It is clearly indicated that the ΔE value was considerably decreased as compared to the ligand ($\Delta E = 9.84$ eV) and all the complexes have the ΔE values in the range 8.21–9.00 eV. In all the studied compounds, the copper and nickel exhibited lower ΔE values and according to the above discussions these two molecules have comparatively more reactive and exhibited higher biological activities against tested pathogens. Further, Figure 2 indicated the electron density located around the metal ions in the complexes which also supports the above results [51, 52].

$$\text{Energy gap } (\Delta E) = E_{\text{HOMO}} - E_{\text{LUMO}} \tag{1}$$

$$\text{Electronegativity } (\chi) = \frac{(I + A)}{2} \tag{2}$$

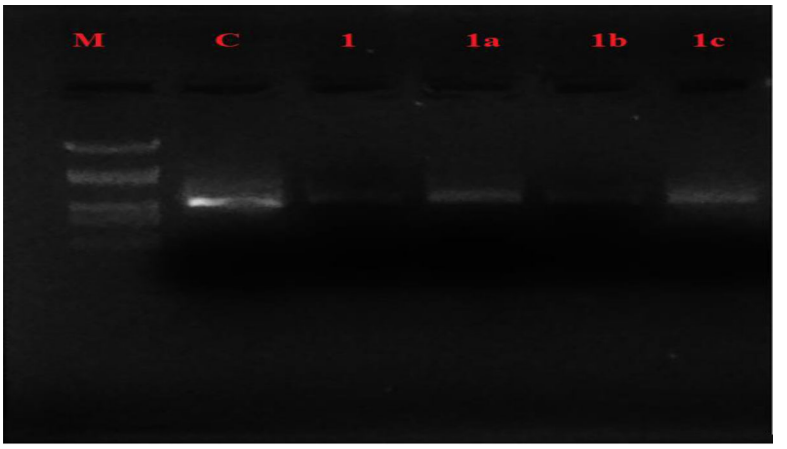

Figure 3. DNA cleavage activity on plasmid pUC18 DNA: **M**: Standard DNA, **C**: Control DNA (untreated pUC 18), **1**: azo dye ligand, **1a**: Cu(II) complex, **1b**: Co(II) complex and **1c**: Ni(II) complex.

$$\text{Chemical potential } (\alpha) = -\frac{(I + A)}{2} \tag{3}$$

$$\text{Hardness } (\eta) = \frac{(I - A)}{2} \tag{4}$$

$$\text{Electrophilicity index } (w) = \frac{\alpha^2}{2\eta} \tag{5}$$

$$\text{Electron affinity } (I) = -E_{LUMO} \tag{6}$$

$$\text{Ionization potential } (A) = -E_{HOMO} \tag{7}$$

3.9. Pharmacological activity results

3.9.1. Antibacterial activity

The newly synthesized azo dye ligand (L) and its Cu(II), Co(II), and Ni(II) complexes were evaluated for their antibacterial studies against three bacterial strains, *E. coli*, *K. pneumoniae*, and *B. subtilis*. The MIC values of the compounds against respective bacterial strains along with the standard are given in Table 8. From the results, it is clear that all the synthesized compounds exhibited promising antibacterial properties against tested bacterial strains. On comparing the antibacterial activity of the ligand and its metal complexes, it is inferred that the metal complexes exhibited more inhibitory effect on the growth of all the microorganisms and this may due to the change in molecular structure due to coordination with the metal ion that tends to make a metal complex act as more powerful and potent bactericidal agents. Thus, the results of the antibacterial activity of the synthesized compounds can be summarized as **1c** > **1a** > **1b** > **1**.

In general, the increase in the antibacterial activity of the complexes over the free ligand could be predicted in the light of "Chelation Theory." The enhancement in the bactericidal activity may be rationalized on the basis that ligands mainly possess azo (-N = N-) group. Moreover, on coordination, the polarity of the metal ion will be greatly reduced due to the overlap of ligand orbitals with metal orbitals and partial

Table 9. The results of the cytotoxic activity of the ligand and its metal complexes (IC_{50}, in μM) by MTT assay.

Compounds		K562	A549	MDA-MB-231
1	L	44.38	>50	>50
1a	$[Cu(L)_2]$	24.18	>50	>50
1b	$[Co(L)_2(H_2O)_2]$	19.31	17.77	>50
1c	$[Ni(L)_2(H_2O)_2]$	25.87	>50	>50
Cisplatin		8.23	7.36	11.68

sharing of the positive charge of the metal ion with the donor groups present in the ligand. Thus, lipophilic character of the central metal ion will increase, which favors its permeation more efficiently through the lipid layer of the microorganism. Further, these complexes completely disturb the respiration process of the cell and thus block the protein synthesis, which restricts further growth of the organisms [53].

3.9.2. DNA-Cleavage activity

Although there has been a wide discovery of drugs for treatment of various diseases, it remained as a challenge that causes most of the human deaths worldwide [54]. This is mainly due to limitations of the drugs such as high toxicity, serious side effects and drug resistance [55]. These limitations that render drugs inability could be associated with their interaction with the DNA. Therefore, DNA-cleavage studies are essential to understanding the mechanism of toxicity of the drugs with the DNA molecule, where DNA-cleavage is controlled by relaxation of circular form of pUC18 DNA into nicked circular form and linear form. When circular plasmid DNA is conducted by electrophoresis the faster migration will be observed for the supercoiled form (Form I). If one strand is cleaved, supercoils will relax to produce a slow moving open circular form (II). If both strands are cleaved, a linear form (Form III) will be generated that migrates in between I and II [56].

In the present study, the cleavage ability of the synthesized compounds on DNA was performed by gel electrophoresis method. The results of the DNA cleavage activity of the ligand and its metal complexes are as shown in Figure 3. These findings indicated that Cu(II) and Ni(II) complexes show complete cleavage of all forms of DNA, whereas ligand and Co(II) complex partially cleaved Form I DNA and completely cleaved Form II DNA compared to control DNA. Further, it can be noted that the control DNA alone did not exhibit any apparent cleavage, whereas the ligand and its metal complexes exhibited cleavage and these could be explained by an important coordination role of nitrogen and oxygen to the metal ions in these isolated DNA cleavage reactions. From the rest of the biological studies like antibacterial and cytotoxic studies carried out in this work have a good correlation with the cleavage properties and therefore it can be evident that the metal ion present in an heterocyclic core can be an efficient pharmacological agent as they exhibited appreciable cleavage properties. This can be interpreted that these studied complexes cleave the genome of the respective microorganisms effectively and thereby inhibit the growth and finally leads to the death of the cells. From these findings, it is apparent that the tested compounds are potential inhibitors for pathogenic microorganisms.

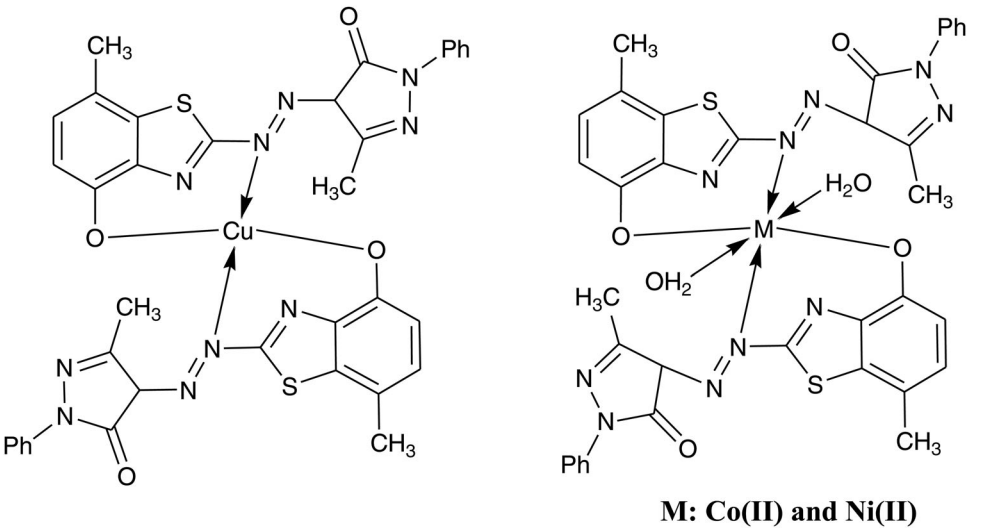

Figure 4. The proposed molecular geometries for the synthesized metal complexes.

3.9.3. Cytotoxic activity results

The anticancer activity of the novel bioactive metal complexes of azo dye containing pyrazole moiety was carried out against some selected cancer cell lines, human chronic myeloid leukemia cell line (K562), human lung carcinoma cell line (A549), and human mammary tumor cell line (MDA-MB-231) by MTT assay. The results of the activity in terms of IC_{50} values (μM) are presented in Table 9. The results indicated that the metal complexes exhibited lower values of IC_{50} against K562 cell line and this suggests that all these metal chelates are proved to be potential anticancer agents. Furthermore, the moderate activity was exhibited by the compounds against A549 and MDA-MB-231 cell lines. From overall observation, it is concluded that the chelation can enhance the pharmacological properties of the compounds by suppressing the anomalous behavior of the cells which do not have any particular physiological functions in the biological system. Also, these types of drugs having metal ions in their structures can destroy the tumors present in the biological system more effectively as compared to the simple heterocyclic compounds. This can be attributed to the discovery of platinum-based molecules ruled the whole drug industry by exhibiting excellent anticancer properties. Therefore, the present compounds can be used in the development of metal-based drugs in the future [57, 58].

4. Conclusion

The present work is focused on the synthesis of novel azo dye ligand 4-[(7-hydroxy-4-methyl-1,3-benzothiazol-2-yl)diazenyl]-5-methyl-2-phenyl-2,4-dihydro-3*H*-pyrazol-3-one (L) and its Cu(II), Co(II) and Ni(II) complexes. All the synthesized compounds were characterized by analytical and spectroscopic techniques. IR spectral data indicate that the azo-dye ligand behaves as a monobasic bidentate O,N-donor coordinating *via* the nitrogen atom of the azo group and oxygen atom of the deprotonated hydroxyl group of the benzothiazole moiety. Magnetic moment and electronic spectra suggest distorted tetrahedral

geometry for Cu(II) complex and octahedral geometry for the Co(II) and Ni(II) complexes. ESR data showed that the complexes are mononuclear in nature. Based on the analytical and spectroscopic results, the following structures were proposed for the complexes and they are presented in Figure 4. The molecular structures of the synthesized compounds were analyzed by quantum chemical technique (ZINDO/1) and the optimized structures were used for the interpretation of chemical reactivity. The antibacterial activity results showed that all the metal complexes exhibited higher activity against different microbial strains when compared with the free ligand. We have also studied the DNA-cleavage activity of newly synthesized ligand and its metal complexes by gel electrophoresis. All the compounds except ligand (L) and its Co(II) complex cleaved completely by the DNA molecule. From the above observation, it is revealed that the metal chelates of the azo dye ligand having pyrazole ring can be considered as significant anticancer agents.

Acknowledgements

Authors are thankful to the Department of Chemistry, Kuvempu University, Shankaraghatta, Shimoga for providing the laboratory facilities. We are grateful to the SAIF Panjab University, STIC Cochin University, SAIF IIT Madras for providing spectral and analytical data.

Disclosure statement

No potential conflict of interest was reported by the authors.

References

[1] H. Zollinger. *Azo and Diazo Chemistry*, Vol. **39**, No. 8, Interscience, New York (1961).
[2] H. Zollinger. *Colour Chemistry. Synthesis, Properties, and Applications of Organic Dyes*, VCH, Weinheim (1987).
[3] H. Nishihara. *BCSJ*, **77**, 407 (2004).
[4] R. Gup, E. Giziroglu, B. Kirkan. *Dyes Pigm.*, **73**, 40 (2007).
[5] T. Sasaki, J.M. Tour. *Org. Lett.*, **10**, 897 (2008).
[6] W.R. Browne, B.L. Feringa. *Annu. Rev. Phys. Chem.*, **60**, 407 (2009).
[7] M.S. Ho, A. Natansohn, P. Rochon. *Macromolecules*, **28**, 6124 (1995).
[8] A. Ni, K. Chen, H. Tian. *Dyes Pigm.*, **50**, 13 (2001).
[9] S. Yoopensuk, P. Tongying, K. Hansongnern, C. Pakawatchai, S. Saithong, Y. Tantirungrotechai, N. Leesakul. *Spectrochim. Acta A Mol. Biomol. Spectrosc.*, **86**, 538 (2012).
[10] T. Nakamura, R.R. Bommu, Y. Kamshi, T. Shibusawa. *Textile Res. J.*, **70**, 80 (2000).
[11] R. Bianchini, G. Catelani, R. Cecconi, F. D'Andrea, E. Frino, J. Isaad, M. Rolla. *Carbohydr. Res.*, **343**, 2067 (2008).
[12] D.P.S. Rathore, M. Kumar, P.K. Bhargava. *Chem. Anal.*, **40**, 805 (1995).
[13] N.M. Mallikarjuna, J. Keshavayya, M.R. Maliyappa, R.A. Shoukat Ali, T. Venkatesh. *J. Mol. Struct.*, **1165**, 28 (2018).
[14] N.M. Mallikarjuna, J. Keshavayya. *JKSUS*, **32**, 251 (2020).
[15] N.M. Mallikarjuna, J. Keshavayya, B.N. Ravi. *J. Mol. Struct.*, **1173**, 557 (2018).
[16] M.N. Matada, K. Jathi. *J. Coord. Chem.*, **72**, 1994 (2019).
[17] M.R. Maliyappa, J. Keshavayya, N.M. Mallikarjuna, P.M. Krishna, N. Shivakumara, T. Sandeep, K. Sailaja, M.A. Nazrulla. *J. Mol. Struct.*, **1179**, 630 (2019).
[18] M.R. Maliyappa, J. Keshavayya, M. Mahanthappa, Y. Shivaraj, K.V. Basavarajappa. *J. Mol. Struct.*, **1199**, 126959 (2020).

[19] N.M. Mallikarjuna, J. Keshavayya, B.M. Prasanna, B.M. Praveen, H.C. Tandon. *J. Bio. Tribocorros.*, **6**, 1 (2020).
[20] M.N. Matada, K. Jathi, P. Malingappa, I. Pushpavathi. *CDC*, **25**, 100314 (2020).
[21] J. Mendham, R.C. Denney, J.D. Barnes, M.J.K. Thomas. *Vogel's Quantitative Chemical Analysis*, 6th edn, Prentice Hall, London (2000).
[22] V. Asati, N.K. Sahu, A. Rathore, S. Sahu, D.V. Kohli. *Arab. J. Chem.*, **8**, 495 (2015).
[23] S. Sarkar, J. Dwivedi, R. Chauhan. *J. Pharm. Res.*, **7**, 439 (2013).
[24] P.A. Wayne. *Methods for Dilution Antimicrobial Susceptibility Tests for Bacteria that Grow Aerobically; Approved Standard*, M7, 7th Edn. Clinical and Laboratory Standards Institute, CLSI, Wayne, Pennsylvania, USA (2006).
[25] J. Gutierrez, C. Barry-Ryan, P. Bourke. *Food Microbiol.*, **26**, 142 (2009).
[26] Z. Schelz, J. Molnar, J. Hohmann. *Fitoterapia*, **77**, 279 (2006).
[27] S.J. Kirubavathy, S. Chitra. *J. Mol. Struct.*, **1147**, 797 (2017).
[28] J. Sambrook, E.F. Fritsch, T. Maniatis. *Molecular Cloning; A Laboratory Manual*, 2nd edn, Cold Spring Harbor Laboratory Press, Cold Spring Harbor, New York, USA (1989).
[29] A. Doyle, J.B. Griffiths (Eds.). *Cell and Tissue Culture for Medical Research*, Wiley, New York, USA (2000).
[30] M.N. Matada, K. Jathi. *J. Mol. Struct.*, **1180**, 196 (2019).
[31] W.J. Geary. *Coord. Chem. Rev.*, **7**, 81 (1971).
[32] M. Gaber, A.M. Hassanein, A.A. Lotfalla. *J. Mol. Struct.*, **875**, 322 (2008).
[33] N.T. Abdel-Ghani, A.M. Mansour, M.F.A. El-Ghar, O.M. El-Borady, H. Shorafa. *Inorg. Chim. Acta*, **435**, 187 (2015).
[34] P. Singh, A.K. Singh, V.P. Singh. *Polyhedron*, **65**, 73 (2013).
[35] A.M.A. Alaghaz, M.E. Zayed, S.A. Alharbi. *J. Mol. Struct.*, **1084**, 36 (2015).
[36] M.S. Masoud, S.S. Hagagg, A.E. Ali, N.M. Nasr. *J. Mol. Struct.*, **1014**, 17 (2012).
[37] S.A.A. El-Enein, S.M. Emam, M.W. Polis, E.M. Emara. *J. Mol. Struct.*, **1099**, 567 (2015).
[38] S.N. Chaulia. *J. Chem. Pharm. Res.*, **8**, 242 (2016).
[39] Q. Peng, M. Li, K. Gao, L. Cheng. *Dyes Pigm.*, **14**, 89 (1990).
[40] W. You, H. Zhu, W. Huang, B. Hu, Y. Fan, X. You. *Dalton Trans.*, **39**, 7876 (2010).
[41] N. Raman. *Russ. J. Coord. Chem.*, **35**, 234 (2009).
[42] A.A. El-Bindary, A.Z. El-Sonbati, A.F. Shoair, A.S. Mohamed. *J. Mol. Liq.*, **220**, 409 (2016).
[43] A.Z. El-Sonbati, I.M. El-Deen, M.A. El-Bindary. *J. Mol. Liq.*, **215**, 612 (2016).
[44] A.Z. El-Sonbati, M.A. Diab, A.A. El-Bindary, M.I. Abou-Dobara, H.A. Seyam. *Spectrochim. Acta A Mol. Biomol. Spectrosc.*, **104**, 213 (2013).
[45] T.S. Rao, K.L. Reddy, P. Lingaiah. *Proc. Indian Acad. Sci. (Chem. Sci.)*, **100**, 363 (1998).
[46] A.M.A. Alaghaz, M.E. Zayed, S.A. Alharbi, R.A.A. Ammar, A. Elhenawy. *J. Mol. Struct.*, **1084**, 352 (2015).
[47] I. Georgieva, N. Trendafilova, G. Bauer. *Spectrochim. Acta A Mol. Biomol. Spectrosc.*, **63**, 403 (2006).
[48] M. Gaber, K.Y. El-Baradie, Y.S.Y. El-Sayed. *Spectrochim. Acta A Mol. Biomol. Spectrosc.*, **69**, 534 (2008).
[49] M. Gaber, Y.S. El-Sayed, K. El-Baradie, R.M. Fahmy. *J. Mol. Struct.*, **1032**, 185 (2013).
[50] M.S. Alam, D. Lee. *J. Mol. Struct.*, **1128**, 174 (2017).
[51] B. Kosar, C. Albayrak. *Spectrochim. Acta A Mol. Biomol. Spectrosc.*, **78**, 160 (2011).
[52] N. Sinha, O. Prasad, V. Narayan, A.R. Shukla. *J. Mol. Simul.*, **37**, 153 (2011).
[53] J. Joseph, G. Ayisha Bibin Rani. *Arab. J. Chem.*, **10**, 1963 (2017).
[54] S.H. van Rijt, P.J. Sadler. *Drug Discov. Today*, **14**, 1089 (2009).
[55] P.C.A. Bruijnincx, P.J. Sadler. *Curr. Opin. Chem. Biol.*, **12**, 197 (2008).
[56] A.K. Patra, T. Bhowmick, S. Roy, S. Ramakumar, A.K. Chakravarty. *Inorg. Chem.*, **48**, 2932 (2009).
[57] M. Kumar, K. Ramasamy, V. Mani, R.K. Mishra, A.B.A. Majeed, E. De Clercq, B. Narasimhan. *Arab. J. Chem.*, **7**, 396 (2014).
[58] T.R. Bal, B. Anand, P. Yogeeswari, D. Sriram. *Bioorg. Med. Chem. Lett.*, **15**, 445(2005).